

Dijital Fotogrametri Tabanlı Başlangıç Kusurlarının Gemi Tipi Desteklenmiş Levhaların NLFEM ile Nihai Mukavemet Analizlerinde Kullanılabilirliğinin İncelenmesi

Hasan Ölmez

Gemi Makinaları İşletme Mühendisliği Bölümü, Sürmene Deniz Bilimleri Fakültesi, Karadeniz Teknik Üniversitesi, Trabzon, Türkiye

hasanolmez@ktu.edu.tr, ORCID: 0000-0001-5351-4046

ÖZET

Bu çalışmada, başlangıç sehimlerinin gemi tipi desteklenmiş panel yapılarının nihai mukavemet değerleri üzerindeki etkileri, başlangıç sehim formlarının nasıl elde edildiği açısından ele alınmış ve analiz edilmiştir. Gemilerdeki desteklenmiş paneller, operasyonel ömürleri boyunca karmaşık yükleme koşullarına maruz kalmakta ve yapısal bütünlüklerinin korunmasını kaçınılmaz hale getirmektedir. Mukavemetlerinin ve göçme modlarının doğru bir şekilde tahmin edilmesi, çeşitli kusurların davranışları üzerindeki etkilerinin kapsamlı bir şekilde anlaşılmasını gerektirir. Bu çalışmada, başlangıç kusurlarının iki temel kaynağı ele alınmıştır. Bunlar, doğrusal öz değer burkulma analizi sonuçları ve dijital fotogrametri tabanlı ölçümler sonucunda ortaya çıkan burkulma modu şekilleridir. Üretim sürecinden kaynaklanan burkulma modu şekilleri, doğrusal statik yapısal analiz kullanılarak elde edilmiştir. Öte yandan, fiziksel yapının yüksek çözünürlüklü görüntülerini analiz ederek kusurları yakalamak ve ölçmek için dijital fotogrametri kullanılmıştır. Sayısal hesaplamalar, bu iki tür başlangıç kusurunun doğrusal olmayan sonlu elemanlar yöntemi (NLFEM) analizlerine dahil edilmesiyle gerçekleştirilmiştir. Burkulma modu kusurları geometrik düzensizlikler olarak uygulanırken, fotogrametri tabanlı kusurlar ideal geometriden istatistiksel olarak temsili sapmalar olarak elde edilmiştir. Desteklenmiş panelin yapısal davranışı, boyuna tek eksenli basınç yüklemesi altında analiz edilmiştir. Ansys 2019R2 versiyonundan itibaren artık kullanılmayan Türk Loydu'nun S.P 01/19 teknik genelgesinde verilen prosedür yerine yeni bir NLFEM proje şeması kullanılmıştır. Önerilen bu yöntemin geçerliliği, Ansys 2022R2 versiyonunda, burkulma modu başlangıç kusurlarını dikkate alan iki doğrulama çalışması ile kanıtlanmıştır. Daha sonra, Trabzon'daki bir tersanede imal edilen modelden dijital fotogrametri yöntemi ile Photomodeler V. 2023.3.0.238 programında oluşturulan desteklenmiş panel yapısı için bir uygulama çalışması yapılmıştır. NLFEM analizi, hem öz değer burkulma analizinden sonra elde edilen başlangıç sehimleri modeli ile hem de kaynak montaj işlemlerinden sonra doğal olarak yapısal bozulmalara uğramış model için gerçekleştirilmiştir. Karşılaştırmalı nihai mukavemet sonuçları oldukça tutarlı belirlenmiş ve bu da dijital fotogrametrik modelleme yönteminin gemi yapı elemanlarının mukavemet analizinde kullanılabileceğini göstermiştir.

Anahtar kelimeler: Gemi mukavemeti, desteklenmiş levha, başlangıç kusurları, nihai mukavemet, NLFEM, Dijital Fotogrametri

Makale geçmişi: Geliş 06/11/2023 – Kabul 03/01/2024

<https://doi.org/10.54926/gdt.1386576>

Evaluation of the Applicability of Digital Photogrammetry-Based Initial Imperfections on NLFEM Ultimate Strength Analysis of Ship-Type Stiffened Plates

Hasan Ölmez

Department of Marine Engineering, Sürmene Faculty of Marine Science, Karadeniz Technical University, Trabzon, Türkiye

hasanolmez@ktu.edu.tr, ORCID: 0000-0001-5351-4046

ABSTRACT

In this study, the effects of initial imperfections on the ultimate strength values of ship-type stiffened plate structures are discussed and analysed from the point of view of how the initial imperfection forms are obtained. Ship stiffened panels are subjected to complex loading conditions during their operational lifespan. Accurate prediction of their strength and failure modes necessitates a thorough understanding of the effects of various imperfections on their behavior. Two primary sources of initial imperfections are considered: the buckling mode shapes resulting from linear eigenvalue buckling analysis and measurements based on digital photogrammetry. Buckling mode shapes, arising from the manufacturing process are extracted using linear static structural analysis. Digital photogrammetry is employed to capture and quantify imperfections by analysing high-resolution images of the physical structure. Numerical investigation is conducted by incorporating these two types of initial imperfections into non-linear finite element method (NLFEM) calculations. The buckling mode imperfections are applied as geometric perturbations, while the photogrammetry-based imperfections are incorporated as statistically representative deviations from the ideal geometry. Stiffened panel's structural response is analysed under longitudinal uniaxial compression. A new NLFEM project schematic has been utilized instead of the procedure outlined in the technical circular S.P 01/19 by Türk Loydu, which has been discontinued after ANSYS® Workbench™V.2019R2. This is proven by two validation case studies in ANSYS® Workbench™2022R2 version for considering buckling mode initial imperfections. A case study is then conducted using a 3D model of a stiffened plate panel, which is fabricated in a shipyard located in Trabzon, created by Photomodeler V. 2023.3.0.238 employing the digital photogrammetry method. NLFEM analysis is carried out for both initially deflected model after eigenvalue buckling analysis and naturally deflected model after welding operations. The comparative ultimate strength results are quite consistent, and this shows that the digital photogrammetric modelling method can be used in the analysis of ship structural elements.

Keywords: Ship strength, stiffened plate, initial imperfection, ultimate strength, NLFEM, Digital Photogrammetry

Article history: Received 06/11/2023 – Accepted 03/01/2024

1. Introduction

Ship structures are vital components of the global maritime industry, serving as the backbone of international trade and transportation. The design and analysis of these structures are of paramount importance to ensure their safe and efficient operation. The focus of these studies is the accurate prediction of their structural strength, particularly in the context of nonlinear finite element method (NLFEM) analyses. Accurate predictions require an in-depth understanding of the complex factors that influence the behaviour of ship-type stiffened panels, including the incorporation of realistic residual stresses, boundary conditions and initial imperfections (Paik et al., 2009; Khan and Zhang, 2011; Xu et al., 2013; Tanaka et al., 2014; Yao and Fujikubo, 2016; Kim et al., 2017; Ozdemir et al., 2018; Kim et al., 2018; Li et al., 2021; Tekgoz and Garbatov, 2021).

Ship and offshore structures inevitably display deviations from ideal geometry in the out-of-plane dimension, resulting from processes such as welding, cutting, and manufacturing. These imperfection patterns tend to be highly irregular and, in many cases, lack comprehensive documentation. The structural integrity, particularly concerning buckling and ultimate strength, is notably influenced by the presence of these initial imperfections. In practical terms, classification society standards specify maximum permissible thresholds for out-of-plane variations but do not prescribe specific constraints on the nature or shape of these imperfections. From the start of the study of ultimate strength calculations of single and stiffened plates, many researchers have studied the effects of initial imperfections, proposing design methods and equations to predict the ultimate strength (Kim et al., 2018; Yi et al., 2020; Georgiadis et al., 2021; Ringsberg et al., 2021; Li et al., 2022).

Although finite element (FE) modelling is a prevalent tool for evaluating the ultimate strength of structural systems, the incorporation of non-linear distortions and imperfections into FE models remains a persistent challenge. Two prevalent methods for introducing initial imperfections in NLFEM analyses of ship-type stiffened panels have gained recognition in the maritime engineering community. First one is the use of buckling mode shapes obtained from linear buckling analyses and other one is the application of numerical photogrammetry techniques to capture as-built imperfections directly from physical structures. These methods have unique advantages and challenges, and their comparative analysis can show the accuracy and appropriateness of each approach.

One commonly employed method for incorporating initial imperfections is the use of buckling mode shapes derived from linear buckling analyses. This approach assumes that the critical imperfections correspond to the eigenmodes of the linearized problem and are therefore representative of the overall behaviour. Numerous studies have explored the applicability of this method and its limitations, highlighting issues related to the accuracy of mode shape assumptions and the fundamental simplifications of linear analyses (Paik et al., 2002; Georgiou, 2019; Türk Loydu, 2019).

In contrast, the use of numerical photogrammetry techniques to capture as-built imperfections has emerged as a promising alternative. This method utilizes advanced digital imaging and measurement technologies to obtain high-fidelity representations of the actual geometries of ships and their components for re-engineering purposes (Koelman, 2010; Kolyvas et al., 2015; Tepegöz, 2019) and also structural integrity analysis of ship-type stiffened panels (Chen et al., 2011; Barcelo, 2012; Mouhat et al., 2013; Cubells et al., 2014; Zhang, 2015; Woloszyk et al., 2020, Woloszyk et al., 2021, Graves et al., 2023).

This manuscript presents a systematic investigation into the effects of these two distinct approaches for modelling initial imperfections in NLFEM strength analysis. Specifically, we compare the traditional use of buckling mode shapes with the innovative use of numerical photogrammetry-based

imperfections. Despite the growing body of research on these two approaches, a comprehensive comparison of their effects on NLFEM strength analysis of ship-type stiffened panels is notably lacking in the literature. This manuscript aims to provide useful info about the positive and negative sides of both methods and contributes to the advancement of best practices in structural analysis and design for maritime applications. In this context, a 3-step procedure is proposed, incorporating the scaling factor within the eigenvalue buckling analysis section of ANSYS® Workbench™ NLFEM, rather than utilizing the previously employed 5-step procedure. Besides, a reliable and practical procedure (ANSYS® Workbench™, 2022) by utilizing photogrammetry technique (PhotoModeler, 2023) is proposed.

2. Problem Definition and Applied Methods

This research is dedicated to the modeling and examination of imperfect structures through the application of actual dimensions, using the photogrammetry method especially used in geodesical field. This investigation emphasizes the reliability of photogrammetric measurements in assisting with the structural assessment of imperfect segments within ship stiffened plates. Initially, the digital photogrammetry technique is employed to capture the naturally deflected stiffened plates following assembly operations. The initially imperfect model of the stiffened plate created by digital photogrammetry is then transferred to a finite element model and ultimate strength is calculated with directly non-linear static structural analysis. In addition, the ultimate strength analysis of stiffened plates considering first mode buckling imperfections modelling techniques is conducted with linear static structural, eigenvalue buckling and non-linear static structural modules, respectively.

2.1. Ultimate strength analysis of stiffened plates

Ship structures are primarily characterized by their composition of steel plates and stiffeners, meticulously assembled to create panels that serve as fundamental structural elements. Their prominence in maritime construction can be attributed to the relative ease of fabrication and the exceptional strength-to-weight ratio they offer. Throughout the operational lifecycle of vessels, these panels are subject to the application of axial loads and bending moments, rendering the structural framework susceptible to potential failure. Notably, a paramount concern pertains to the phenomenon of plate buckling, particularly as it manifests within the context of stiffened panels. Significantly, the understanding of the different behaviors exhibited by these structural constituents remains, at present, incomplete. In order to assess the load-end shortening capacity of these plates, the methodology of the Ultimate Limit State is invoked.

The assessment of the ultimate strength of maritime structures, while considering all plausible failure modes encompassing plate-induced overall buckling, stiffener-induced overall buckling, stiffener tripping, and plate buckling presents a formidable challenge due to the intricate interplay of diverse factors. This complexity arises from the intricate interplay of multifarious factors, including geometric and material attributes, load scenarios, boundary conditions, residual stresses, and out-of-plane initial imperfections post-welding. The material of choice for ship plate fabrication predominantly comprises mild or high tensile steel, often configured in square or rectangular geometries. Loading considerations encompass in-plane loading, distributed lateral loading attributable to hydrostatic pressures, or a combination thereof. The nature of boundary conditions is intrinsically tied to the structural design and variably contingent upon the specific placement of the plate within the overarching structural

framework. Of these considerations, the major emphasis of this study centers on the important assessment of out-of-plane initial imperfections.

2.2. Digital Photogrammetry approach

Photogrammetry, utilizing a three-dimensional measurement approach and central projection imaging as its foundational mathematical framework, has proven to be a highly effective means of gathering data on intricate shapes. It offers consistent measurements over the past few decades and stands as the pioneering remote sensing technology for deducing geometric attributes from photographic images. Automating image processing significantly expedites recognition procedures. Close-range digital photogrammetry is relatively easy to use and provides a high degree of accuracy sufficient for ship structures which allows detailed view of the distortions introduced during the production process or later on during the service life.

Digital methods often offer increased convenience. Digital photogrammetry can be executed without necessitating any preliminary project preparations, like the attachment of specific markers to the object. In the context of digital photogrammetry, the primary emphasis lies in capturing surface irregularities to evaluate examples such as corrosion patterns or other initial depths.

In this study, it is aimed to determine the current structural condition of the supported plate part of a fishing boat under construction according to digital photogrammetric methods by evaluating the photographs taken with a smart phone camera in the PhotoModeler programme and then to compare the results of the analysis with the intact model in the project, which is the basis for the manufacturing layouts.

2.3. Linear and non-linear Finite Element Analysis

Non-linear finite element analysis (NLFEA) currently stands as the cutting-edge and acknowledged methodology for the more accurate prediction of the ultimate strength and buckling behaviors in stiffened panels. However, besides the complex application procedure, NLFEA also requires precise consideration of influential factors such as boundary conditions and formulation of initial imperfections. Therefore, it becomes imperative to develop specialised procedures to ensure a problem-specific and reliable application of NLFEA. NLFEA analyses are conducted through a three-step process. Initially, a linear static structural (LSS) problem of the model is solved. Based on this solution a linear eigenvalue analysis (LEA) is executed to generate essential data regarding the initial imperfections. These imperfections serve as the driving force for instigating the subsequent nonlinear buckling of the stiffened plate. The eigenmodes derived from the linear buckling analysis are harnessed to prepare the “initially deformed” model, which subsequently serves as the input for the nonlinear analysis. The principal objective of NLFEA revolves around the determination of the panel’s ultimate capacity, synonymous with the collapse load, representing the maximum load value that the panel can endure.

ANSYS® Workbench™ project schematic flowchart for the determination of the ultimate strength of stiffened panels by using NLFEM procedure first proposed by the author in the paper (Sekban et al., 2018) is also given in S.P 01/19 technical circular of Turkish Loyd (Türk Loydu, 2019), which is no longer in use after ANSYS® Workbench™ 2019R2 version was released. Instead, a new project schematic develops and proves by two case studies in ANSYS® Workbench™ 2022R2 version. The comparison of project schematics is given in Figure 1.

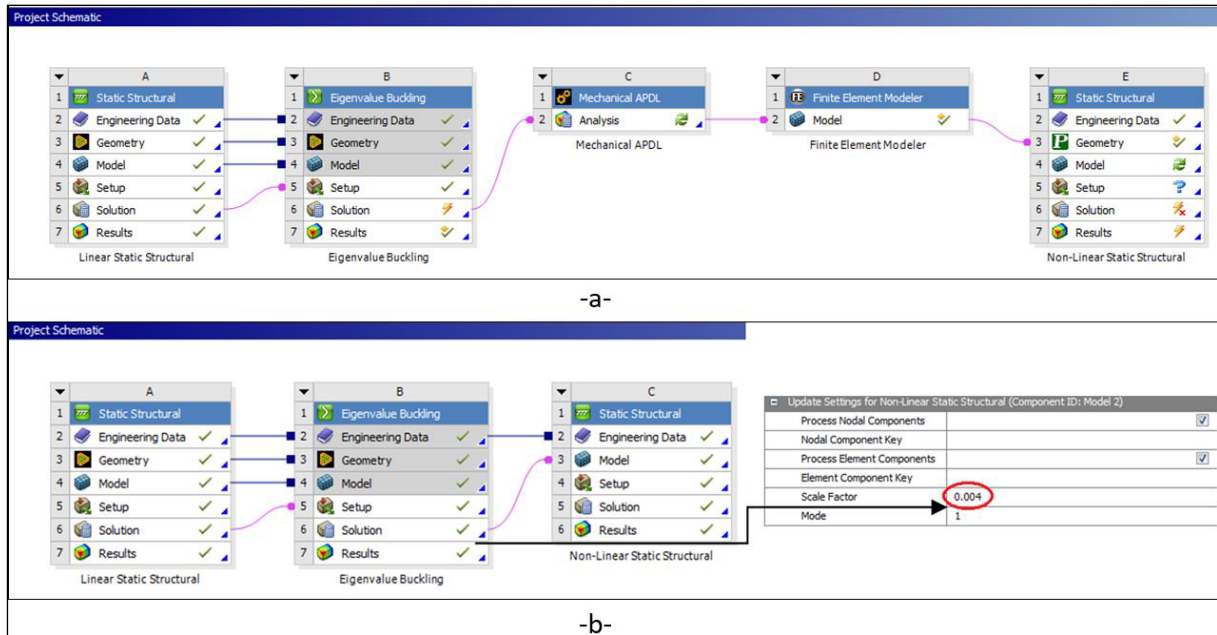


Figure 1. Ultimate strength calculation procedure in ANSYS® Workbench™; a) before ANSYS® Workbench™ 2019R2, b) after ANSYS® Workbench™ 2019R2

3. Validation and Case Studies

Firstly, 3-step ultimate strength calculation procedure of stiffened plate different from S.P 01/19 technical circular of Turkish Loyd is calibrated with analysed stiffened plate models from literature (Quinn et al., 2009; Khan and Zhang, 2011). Then, a 3D model of stiffened plate part fabricated in a shipyard is created both with intact structure and initially deflected structure transferred from photogrammetric model.

3.1. Validation study-I

The first validation study is conducted for aluminium alloy stiffened panel model both tested and simulated after numerical analysis in the paper of (Quinn et al., 2009). The geometrical configuration and material properties are given in Table 1. A rectangular aluminium alloy plate is stiffened with three equally spaced, T-shaped aluminium alloy stiffeners parallel to long side along x-axis. Non-linear isotropic hardening power low behaviour is considered for both plate and stiffener materials. The stiffened plate is considered under longitudinal axial compression load.

Table 1. Geometric and material properties of considered stiffened plate.

B	a	b	t	n_{sx}	h_{wx}	t_{wx}	A_{load}	σ_{Yield}	σ_{YPL}	n	E	
mm	mm	mm	mm		mm	mm	mm ²	MPa	MPa		MPa	
440	590	167	2.2	3	28	2.8	1203.2	324	299	0.406	73700	0.33

A_{load} = Area of loading side including stiffeners, B=plate width, a=plate length, b=plate width between two stiffeners, t=plate thickness, n_{sx} =number of stiffeners, h_{wx} = stiffener web height, t_{wx} = stiffener web thickness, b_{fx} = flange width, t_{fx} = flange thickness, σ_{Yield} = yield stress, σ_{YPL} = Initial yield stress of power low, n= exponent of power low, E= Young's modulus, Poisson's ratio.

Boundary conditions are applied separately for linear and non-linear analysis in accordance with those in the reference publication. Firstly in linear analysis, the clamped type boundary condition is used for loaded edges. Longitudinal edges parallel to stiffeners are taken as free boundary. Besides, to avoid

rigid body motion mid-node of the model is constrained against translation x and y directions and one of the mid-node of the longitudinal unloaded edge is constrained against translational y direction. Secondly, in non-linear analysis, forced displacement type loading is used instead of linear pressure. Equal y-displacement is given at loaded plate edge with stiffeners. Translation at z direction, and rotation at x and z directions are constrained. On the opposite edge, translation at y and z directions, and rotation at x and z directions are constrained. Other boundary conditions are similar with linear eigenvalue analysis. Boundary and loading conditions are also shown in Figure 2.

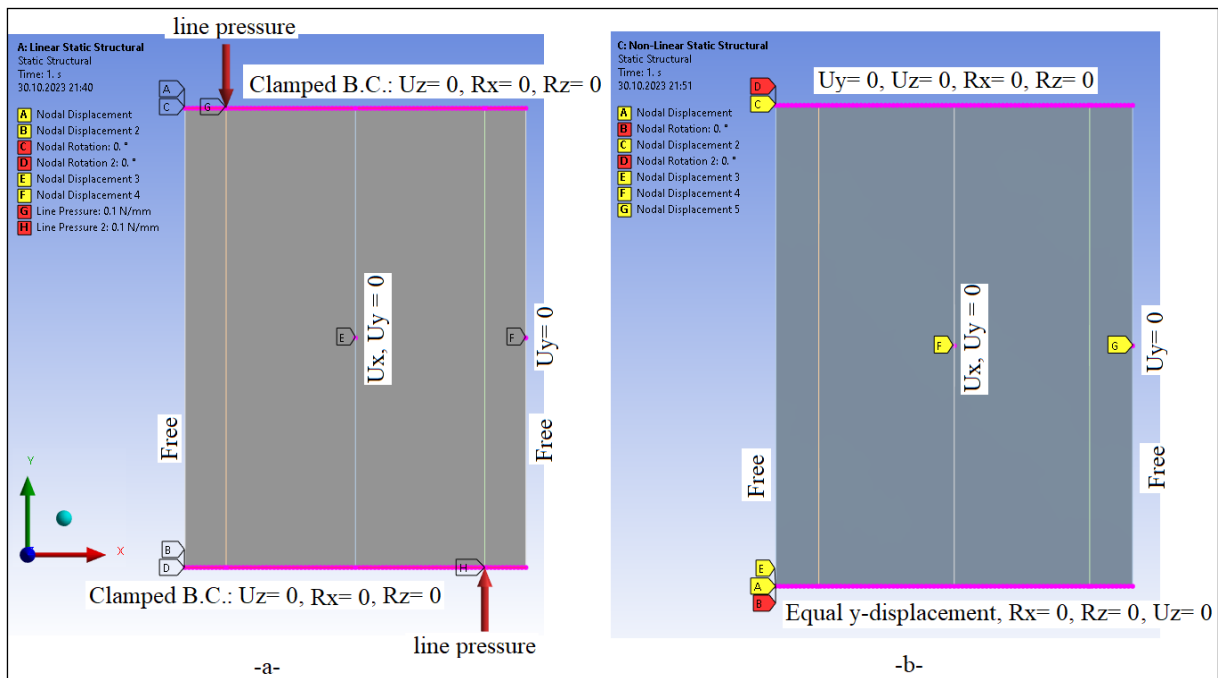


Figure 2. Loading and boundary conditions; (a) Linear static and eigenvalue buckling analysis, (b) Non-Linear static analysis

The optimum numbers of mesh elements for the model parts are determined as 17 elements in the plate between stiffeners, three elements in the stiffener web and 59 elements in the longitudinal edges. Contact configuration and boundary conditions of stiffened plate is given in Figure 3.

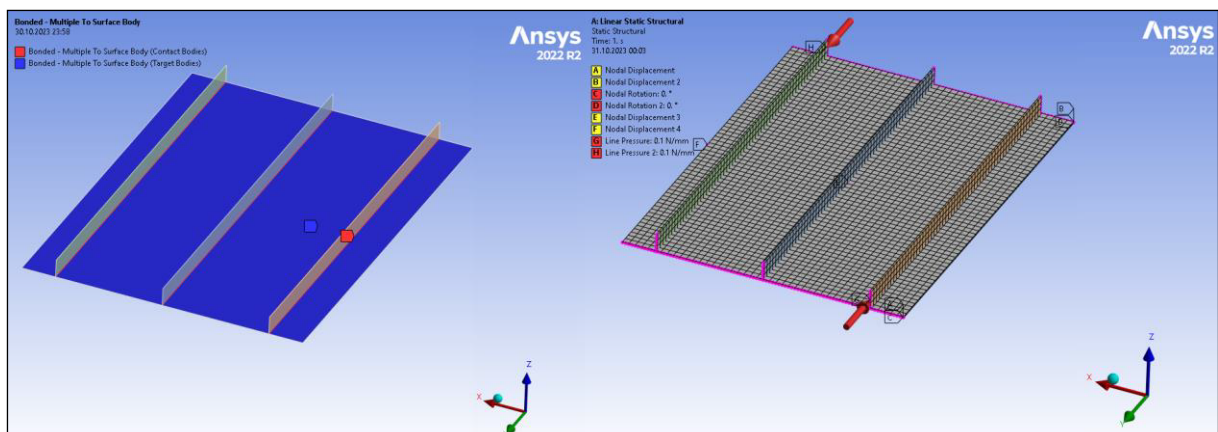


Figure 3. Contact configuration and boundary conditions of stiffened plate.

The 3-step LSS+LEA+NLFEA procedure is carried out and total deformation, equivalent von-Mises stress, and first buckling mode imperfections are obtained and used for NLFEM ultimate strength calculations mentioned in Quinn et al. and ISSC, 2012. The first buckling mode is well matched with literature. Color scaled results are given in Figure 4.

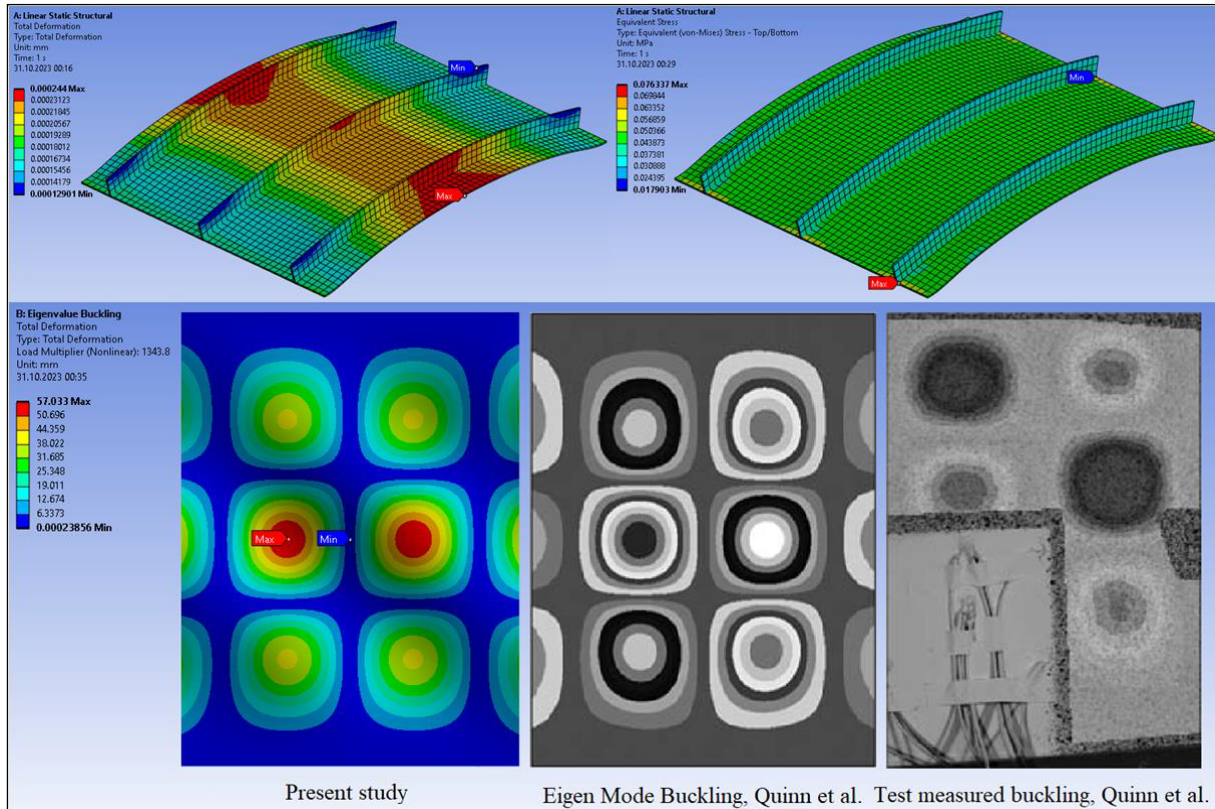


Figure 4. Linear static structural and eigenvalue buckling analysis results

Finally, the load-end shortening curve obtained from NLFEM and comparison graphic is given in Figure 5 and initial plate buckling loads and ultimate plate collapse loads are given in Table 2, comparatively.

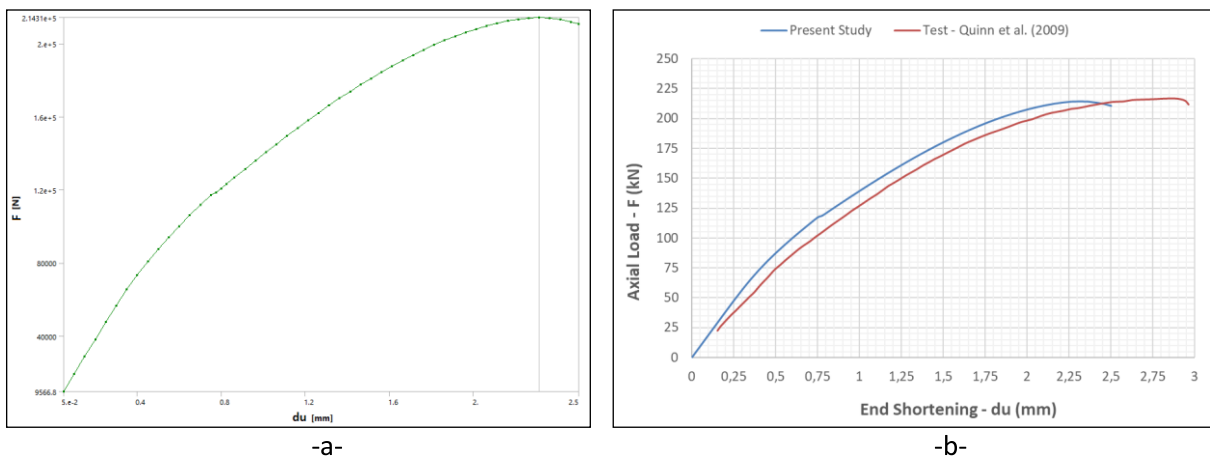


Figure 5. (a) Load-end shortening curve of present study (b) comparative load-end shortening curve

Since the use of different software, different iterative technique under solution module, the comparison to the referenced publication is regarded as satisfactory. Reliable results were obtained

with a difference of about 1,07% ultimate load capacity according to the result of test procedure by Quinn et al., 2009 and 1,23% according to the NLFEM method by (Quinn et al., 2009). By examining the curve's characteristics, the panel will fail when the applied load is 214,3 kN at 2,5 mm end-shortening along the short edge of the stiffened plate.

Table 2. Initial plate buckling and ultimate plate collapse loads

Study	Initial plate buckling load (kN)	Ultimate panel collapse load (kN)
Experimental data [Quinn et al., 2009]	74,5	216,6
Measured imperfection [Quinn et al., 2009]	78,2	212,1
Eigen-mode imperfection, Abaqus [Quinn et al., 2009]	52,8	211,7
Present study, ANSYS® Workbench™	59,1	214,3

Based on the test findings, the initial buckling of the plate was observed at 74.5 kN, which corresponds to 34% of the ultimate collapse load of the specimens. In this scenario, the central plate bays buckled in an anti-symmetrical manner, forming three longitudinal half-waves. This value is predicted as 52,8, 25% of the ultimate load and 59,1, 27% of the ultimate load by (Quinn et al., 2009) and present study, respectively. Comparative results at collapse level are given in Figure 6.

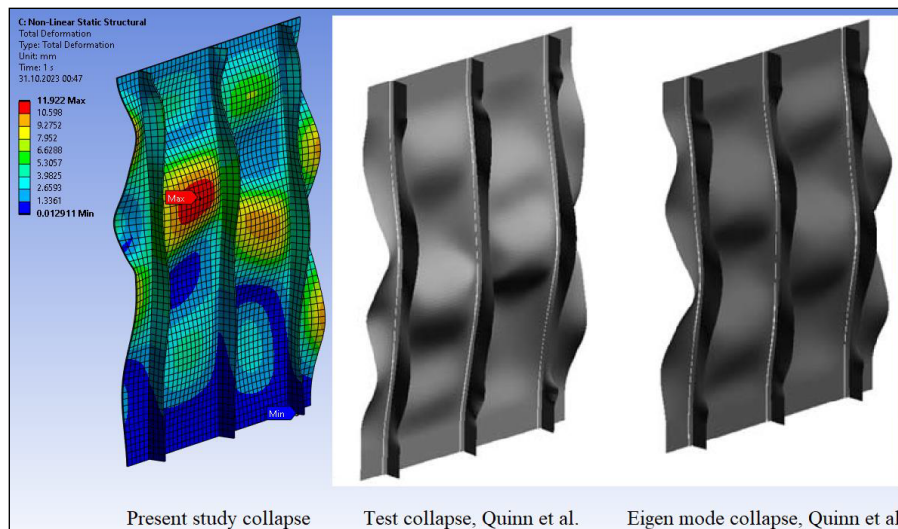


Figure 6. Obtained collapse modes comparison

3.2. Validation study-II

A further comparison study was carried out to strengthen the accuracy and reliability of the proposed procedure. An effort is made to compare ultimate strength results with applicable findings documented by (Khan and Zhang, 2011) and (Türk Loydu S.P 01/19, 2019). The geometrical configuration and material properties are given in Table 3. Almost square steel plate is stiffened with four equally spaced, T-shaped steel stiffeners along the longitudinal x-axis. Bilinear isotropic hardening stress-strain behaviour is considered for both plate and stiffener materials.

The displacement-type boundary conditions, restricted displacements with free rotations, suitable for the stiffened panel's loading edge will be enforced. As a standard practice, the out-of-plane movement of the stiffened panel's edges will be restricted along all plate edges.

Table 3. Geometric and material properties of considered stiffened plate.

B	a	b	t	n_{sx}	h_{wx}	t_{wx}	b_{fx}	t_{fx}	A_{load}	σ_{yield}	ϵ_{yield}	E	E_t	
mm	mm	mm	mm		mm	mm	mm	mm	mm ²	MPa		MPa	MPa	
4075	4300	815	17.8	4	463	8	172	17	99047	315	0.001531	205800	1000	0.3

A_{load} = area of loading side including stiffeners, B=plate width, a=plate length, b=plate width between two stiffeners, t=plate thickness, n_{sx} =number of stiffeners, h_{wx} = stiffener web height, t_{wx} = stiffener web thickness, b_{fx} = flange width, t_{fx} = flange thickness, σ_{yield} = yield stress, ϵ_{yield} = yield strain, E= Young’s modulus, E_t = tangent modulus, Poisson’s ratio.

Likewise, the end cross-section nodes of the stiffeners/frames will undergo identical boundary conditions as those applied to the corresponding plate edges. Since the longitudinal and transverse web frames, which are the primary support elements, exhibit significantly greater rigidity compared to the stiffeners, it is possible to eliminate the structural representation of the frames. Instead, they can be replaced by constraining the displacement in the z-direction of the plate nodes situated along the path of the frame on the plate's surface.

To establish load shortening curves and assess buckling capacity, a controlled displacement is applied by forcing the edge nodes of the model. The resulting compressive force is determined as the reaction force in the opposite direction. The magnitude of the imposed displacement needs to be sufficiently substantial to induce deformations surpassing the ultimate load carrying capacity of the panel. Load application and boundary conditions are given in Figure 7.

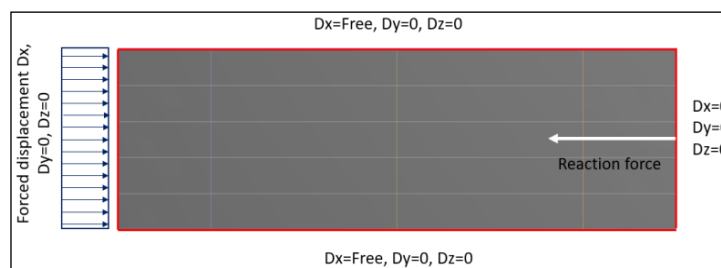


Figure 7. Forced displacement application and boundary conditions

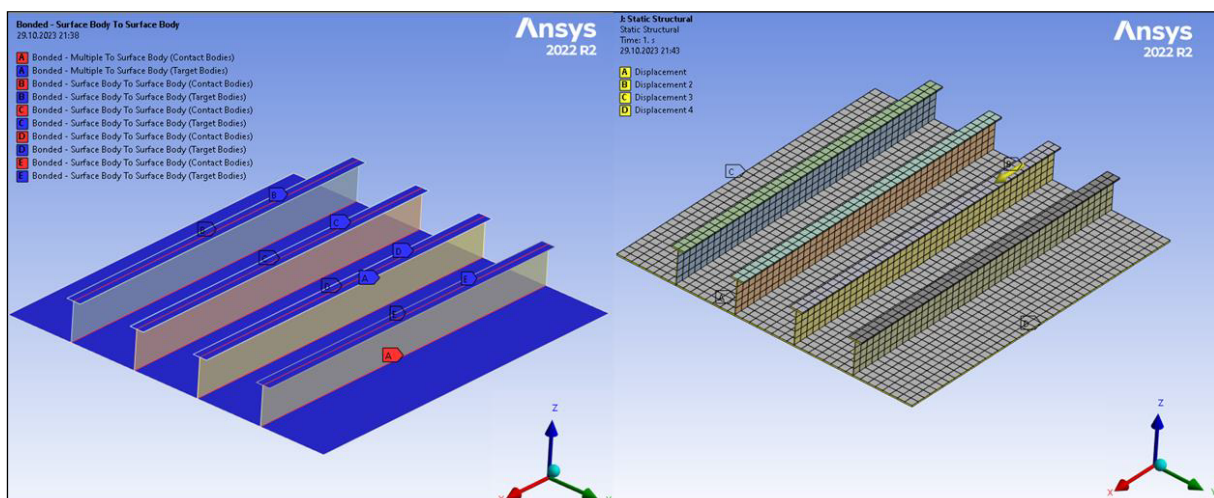


Figure 8. Contact configuration and boundary conditions of stiffened plate.

The optimum numbers of mesh elements for the model parts are determined as eight elements in the plate between longitudinal stiffeners, five elements in the longitudinal stiffener webs, two elements

in the longitudinal stiffener flanges and 44 elements in the longitudinal edges (Lloyd Register, 2016; Türk Loydu S.P 01/19, 2019). Contact configuration and boundary conditions of stiffened plate is given in Figure 8.

The three step LSS+LEA+NLFEA procedure is carried out and total deformation, equivalent von-Mises stress, and first buckling mode imperfections are obtained and color scaled results are given in Figure 9. The first buckling mode is well matched with literature.

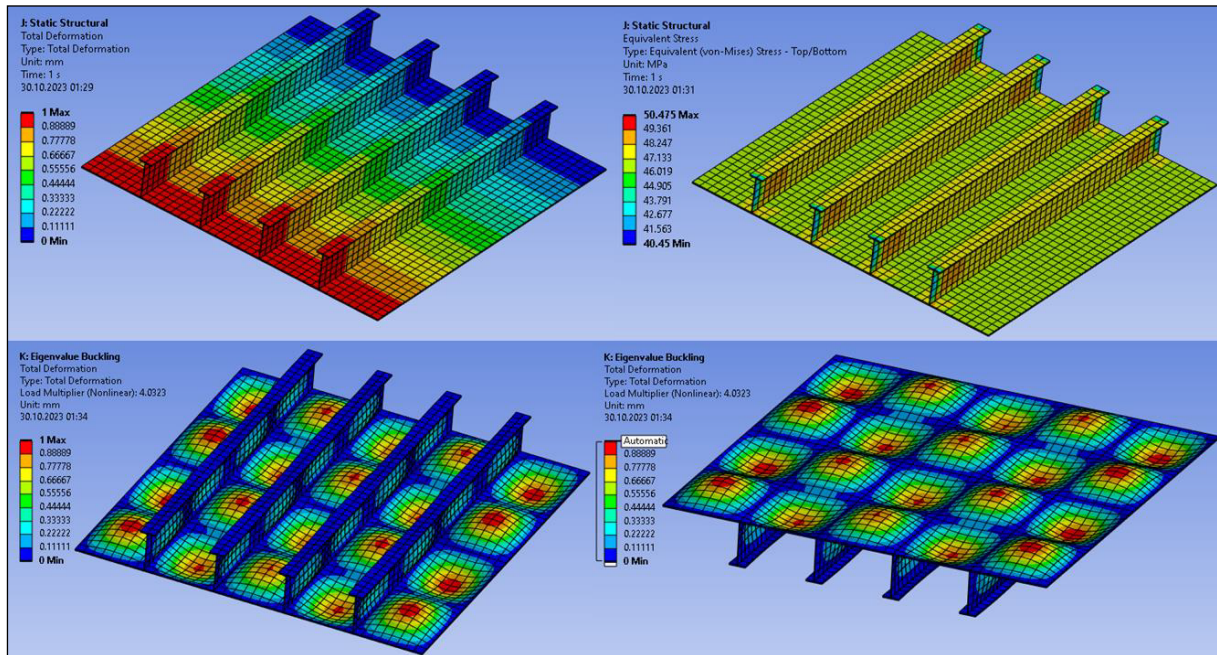


Figure 9. Linear static structural and eigenvalue buckling analysis results

Finally, the load-end shortening curve obtained in this study and comparative normalized stress-strain relations curve graphic are given in Figure 10.

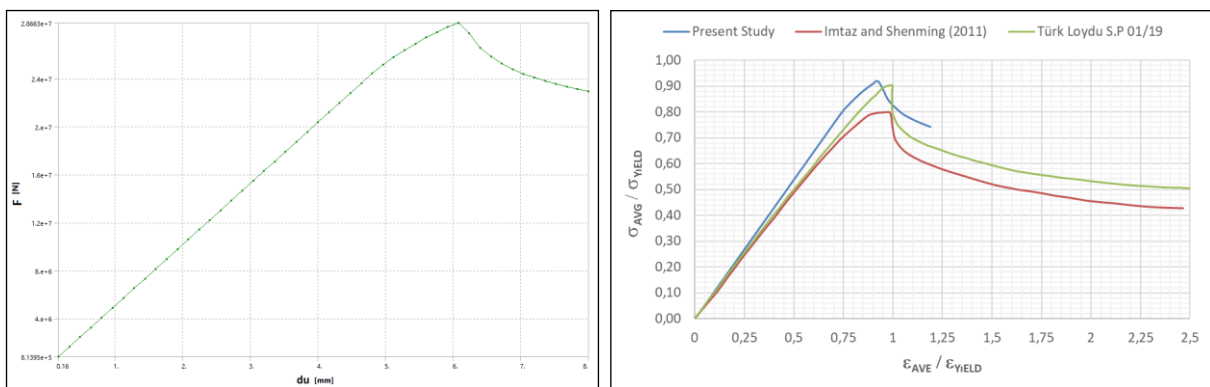


Figure 10. (a) Load-end shortening curve (b) comparative normalized stress-strain relation curve

Given the use of different software, different iterative technique under solution module, distinct initial imperfections and not considering welding-induced residual stress (WRS) effect, the comparison to the referenced publication is regarded as satisfactory. Reliable results were obtained with a difference of 2% ultimate strength according to the result of Türk Loydu procedure and 15% according to the result

obtained by (Khan and Zhang, 2011). By examining the curve's characteristics, it can be deduced that the panel will fail when the average normal compressive stress along the short edge of the stiffened plate comes close to 289 MPa. Equivalent von-Mises stresses at the ultimate state from stiffener and plate side are given in Figure 11.

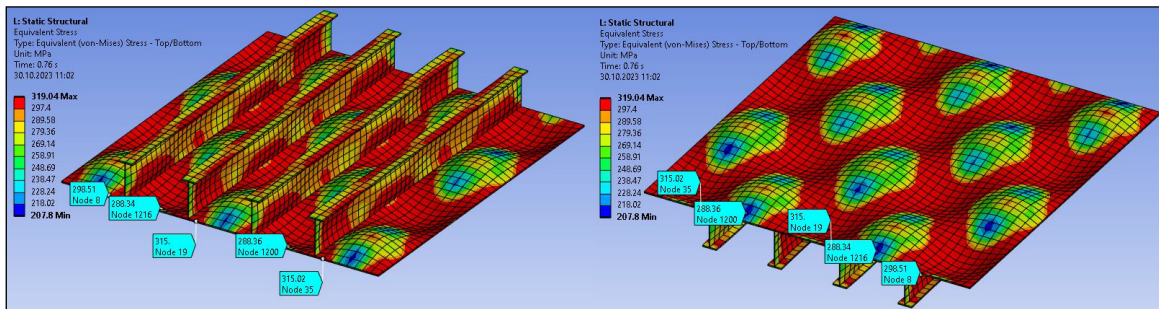


Figure 11. Equivalent von-Mises stresses at the ultimate state from stiffener and plate side.

The welding-induced residual stress (WRS) effect (σ_{rcx}) is not considered in the present study, but considered at the (Khan and Zhang, 2011) results of chosen models for comparison. However, it was reported that 10-13% decrement of ULS of stiffened panel is expected to be achieved due to the effect of welding-induced residual stress, (Khan and Zhang, 2011). In this study, an average level 15,0% decrement was observed as the effect of WRS according to the results obtained without using welding residual induced initial distortions and other factors mentioned above.

3.3. Case Study

A part of stiffened plate from a fishing vessel fabricated in Trabzon shipyard is considered in this part of the study. Firstly, an intact flat model is created in ANSYS® SpaceClaim® and NLFEM analysis is carried out as proposed in validation cases. The geometrical configuration and material properties are given in Table 4. Almost square steel plate is arbitrarily stiffened with an I-type and L-type longitudinal stiffener and L-type transverse web frame. Bilinear isotropic hardening stress-strain behaviour is considered for both plate and stiffener materials. The fabricated part and its FEM model is given in Figure 12.

Table 4. Geometric and material properties of considered stiffened plate.

B	a	b	t	$l_{n_{sx}}$	$l_{h_{wx}}$	$l_{t_{wx}}$	$l_{n_{sx}}$	$l_{h_{wx}}$	σ_{Yield} MPa	E MPa	E_t MPa	0.3
mm	mm	mm	mm		mm	mm		mm				
2290	1509	785	8	1	102,27	10	1	250,4				
$l_{t_{wx}}$	$l_{b_{fx}}$	$l_{t_{fx}}$	$l_{n_{TF}}$	$l_{h_{TF}}$	$l_{t_{TF}}$	$l_{b_{TF}}$	$l_{t_{TF}}$	A_{load}				
mm	mm	mm		mm	mm	mm	mm	mm ²				
8	49,90	8	1	286,4	9	55.5	9	21745				

A_{load} = area of loading side including stiffeners, B=plate width, a=plate length, b=plate width between two stiffeners, t=plate thickness, $l_{n_{sx}}$ =number of I-type stiffener, $l_{h_{wx}}$ = I-type stiffener web height, $l_{t_{wx}}$ = I-type stiffener web thickness, $l_{n_{sx}}$ =number of L-type stiffener, $l_{h_{wx}}$ = L-type stiffener web height, $l_{t_{wx}}$ = L-type stiffener web thickness $l_{b_{fx}}$ = L-type stiffener flange width, $l_{t_{fx}}$ = L-type stiffener flange thickness, $l_{n_{TF}}$ =number of L-type transverse frame, $l_{h_{TF}}$ = L-type transverse frame web height, $l_{t_{TF}}$ = L-type transverse frame web thickness $l_{b_{TF}}$ = L-type transverse frame flange width, $l_{t_{TF}}$ = L-type transverse frame flange thickness, σ_{Yield} = yield stress, E= Young's modulus, E_t = tangent modulus, Poisson's ratio.



Figure 12. Fabricated stiffened plate and FEM model.

Boundary conditions and loading scenario are considered similar to both validation Case 1 and Case 2. The mesh, loading and boundary conditions and von-Mises stress distribution at ultimate stress level are given in Figure 13.

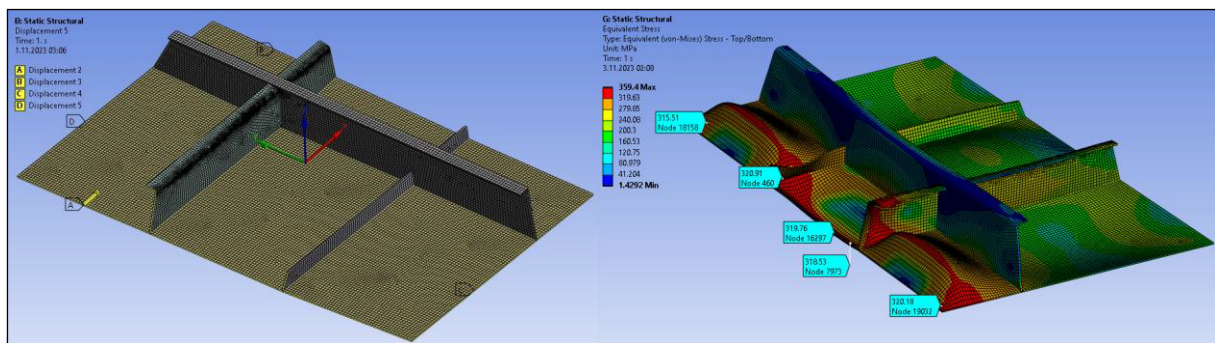


Figure 13. FEM model and von-Mises stress distribution at ultimate level.

Secondly, digital photogrammetry is employed to capture and quantify imperfections by analysing high-resolution images of the physical structure. Numerical investigation is conducted directly one step NLFEM analysis and results are compared to validate the applicability of digital photogrammetry in ship structural analysis. Some user interfaces from Photomodeler is given in Figure 14.

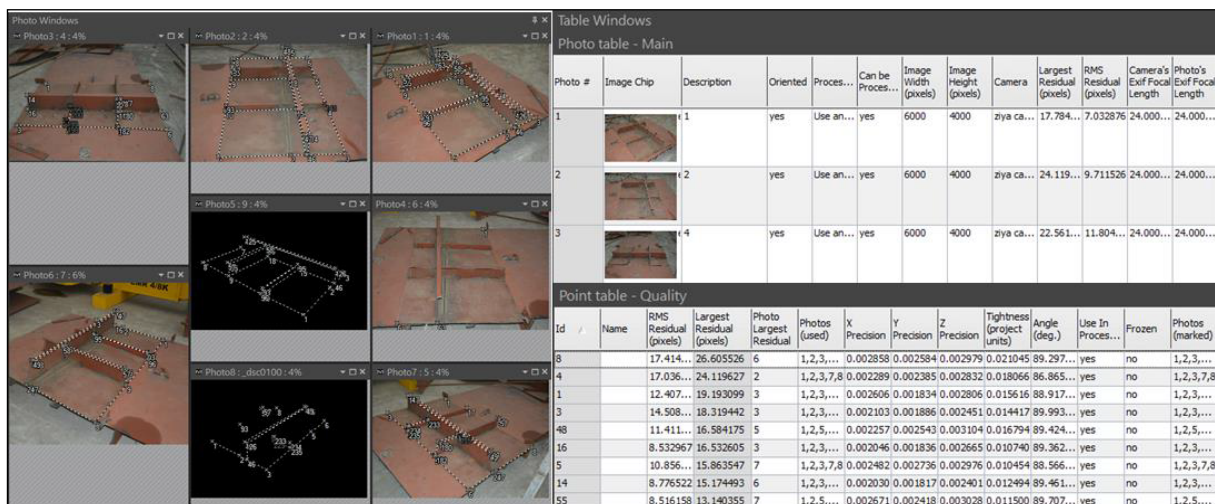


Figure 14. Some of user interfaces from Photomodeler

After Photomodeler studies, a naturally deflected stiffened plate model following assembly operations is obtained and transferred to .dxf / .3dm extension 3D model given in Figure 15.

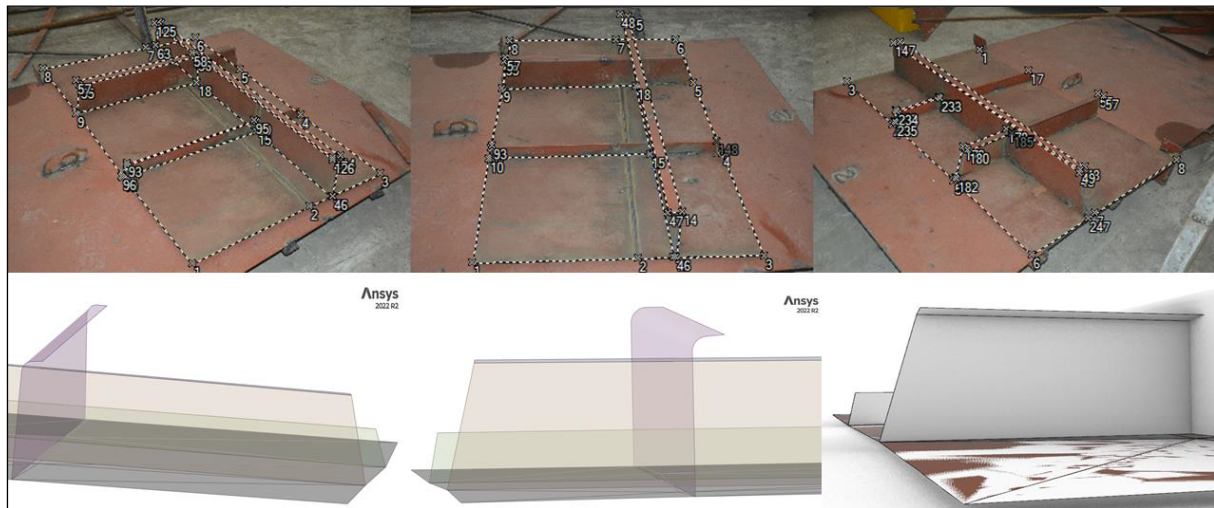


Figure 15. Deflected model transferred to ANSYS® SpaceClaim® module

Boundary conditions and loading scenario are considered similar to both validation Case 1, Case 2 and intact model analysis. The total imperfection and von-Mises stress distribution at ultimate stress level are given in Figure 16.

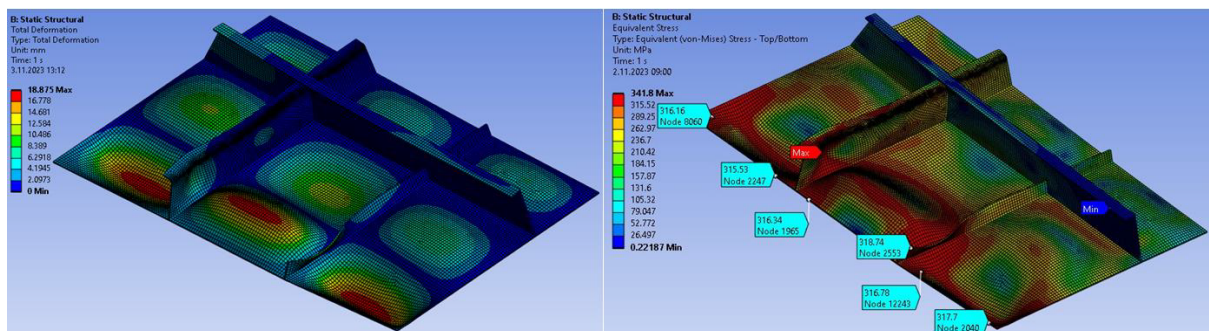


Figure 16. Total imperfection and von-Mises stress distribution at ultimate stress level

As a result, the maximum loads at ultimate strength values were determined quite close to each other. Figure 17 shows the load-end shortening curves of both initially deflected models. The comparative results are also given in Table 5.

4. Results and Conclusions

In this study, the potential of photogrammetry in evaluating the structural integrity of initially deflected ship stiffened plates is highlighted. Stiffened panel's structural response is analysed under longitudinal uniaxial compression loading. A new NLFEM project schematic, which is validated by two case studies in ANSYS® Workbench™ 2022R2 version for considering buckling mode initial imperfections, has been used instead of the procedure given in S.P 01/19 technical circular of Türk Loydu that is no longer in use after ANSYS® Workbench™ 2019R2 version was released. Then a case

study is conducted for 3D stiffened plate created by Photomodeler V. 2023.3.0.238 with digital photogrammetry method from fabricated model in a shipyard in Trabzon. NLFEM analysis is carried out for both initially deflected model after eigen value buckling analysis and naturally deflected model after assembling operations. The main results and conclusions of this study can be summarized as follows:

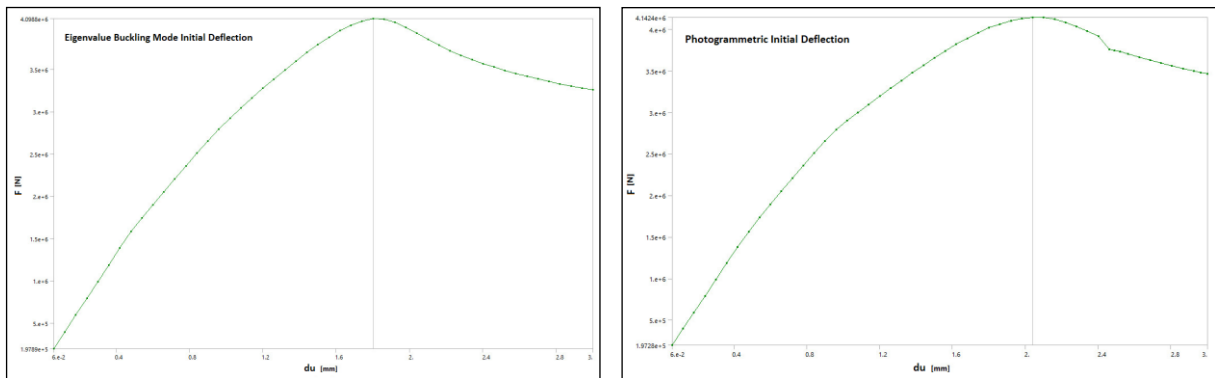


Figure 17. Load – end shortening curves of both models

Table 5. Ultimate plate collapse load and stress results of both models

Method	Ultimate plate collapse load (kN)	ULT (MPa)	ULT/ YIELD
Eigenvalue Buckling Mode Imperfection	4099	188,5	0,598
Photogrammetric Initial Imperfection	4142	190,5	0,605

The 5-step ANSYS® Workbench™ project schematic proposed by Türk Loydu in the “Procedure for the Determination of the Ultimate Strength of Stiffened Panels by Using Non-Linear Finite Element Analysis” is no longer in use after 2019R2 version, because the “Finite Element Modeler” module that provides creation of deformed model is not included in newer versions. Instead of 5-step procedure, a 3-step procedure is proposed with making the scale factor of solution part of eigenvalue buckling analysis determined as 0.004 after trial and error studies in validation study I and validation study II.

After validation study I, reliable results were obtained with a difference of about 1,07% and 1,23% ultimate load capacity according to the result of test procedure and NLFEM method by Quinn et al., 2009, respectively.

After validation study II, reliable results were obtained with a difference of 2% ultimate strength according to the result of Türk Loydu S.P 01/19, 2019 procedure and 15% according to the result obtained by (Khan and Zhang, 2011).

According to validation studies, proposed 3-step ANSYS® Workbench™ analysis technique is reliable and it can be emphasized that Türk Loydu can update their procedure for newer versions of ANSYS® Workbench™.

Ultimate strength results of both models in case study are close to each other with a ratio of 1.06%. Since the comparative ultimate strength results are quite consistent, digital photogrammetric modelling method can be used in the analysis of ship structural elements.

The effects of welding residual stresses and boundary conditions on photogrammetric model analysis results are going to be studied parametrically in next paper.

Besides, a comparison study between Photogrammetric captures and LIDAR captures on corrosion detection and ultimate strength calculations of initially deflected ship-type stiffened plates is going to be planned under a project supported by Karadeniz Technical University.

References

Xu, MC., Yanagihara, D., Fujikubo, M. and Soares, CG. (2013). Influence of boundary conditions on the collapse behaviour of stiffened panels under combined loads. *Marine Structures*, 34, 205-225.

Kim, DK., Lima, HL. and Yua, SY. (2018). A technical review on ultimate strength prediction of stiffened panels in axial compression. *Ocean Engineering*, 170, 392–406.

Li, S., Kim, DK. and Benson, S. (2021). The influence of residual stress on the ultimate strength of longitudinally compressed stiffened panels. *Ocean Engineering*, 231, 1-15.

Khan, I. and Zhang, S. (2011). Effects of welding-induced residual stress on ultimate strength of plates and stiffened panels. *Ships and Offshore Structures*, 6(4), 297–309.

Yao, T. and Fujikubo, M. (2016). *Buckling and ultimate strength of ship and ship-like floating structures*. First edition. Butterworth-Heinemann, Elsevier.

Tanaka, S., Yanagihara, D., Yasuoka, A., Harada, M., Okazawa, S., Fujikubo, M., et al. (2014). Evaluation of ultimate strength of stiffened panels under longitudinal thrust. *Marine Structures*, 36, 21–50.

Paik, JK. And Seo, JK. (2009). Nonlinear finite element method models for ultimate strength analysis of steel stiffened-plate structures under combined biaxial compression and lateral pressure actions–Part II: stiffened panels. *Thin-Walled Structures*, 47, 998–1007.

Ozdemira, M., Ergin, A., Yanagihara, D., Satoyuki Tanaka, S. and Yao, T. (2018). A new method to estimate ultimate strength of stiffened panels under longitudinal thrust based on analytical formulas. *Marine Structures*, 59, 510–535.

Tekgoz, M. and Garbatov, Y. (2021). Collapse strength of intact ship structures. *Journal of Marine Science and Engineering*, 9, 1-20.

Kim, DK., Lima, HL., Kim, MS., Hwanga, OJ. and Park, KS. (2017). An empirical formulation for predicting the ultimate strength of stiffened panels subjected to longitudinal compression. *Ocean Engineering*, 140, 270–280.

Kim, DK., Poh, BY., Lee, JR. and Paik, JK. (2018). Ultimate strength of initially deflected plate under longitudinal compression: Part I = An advanced empirical formulation. *Structural Engineering and Mechanics*, 68(2), 247-259.

Li, S., Georgiadis, DG., Kim, DK. and Samuelides, MS. (2022). A comparison of geometric imperfection models for collapse analysis of ship-type stiffened plated grillages. *Engineering Structures*, 250, 1-13.

Georgiadis, DG., Samuelides, MS., Li, S., Kim, DK., Benson, S., Amdahl, J. and Guedes Soares, C. (2021). Influence of stochastic geometric imperfection on the ultimate strength of stiffened panel in compression. *Developments in the Analysis and Design of Marine Structures*. Taylor & Francis.

Yi, MS., Lee, DH., Lee, HH. and Paik, JK. (2020). Direct measurements and numerical predictions of welding-induced initial deformations in a full-scale steel stiffened plate structure. *Thin-Walled Structures*, 153, 1-17.

Ringsberg, JW., Darie, I., Nahshon, K., Shilling, G., Vaz, MA., Benson, S., et al. (2021). The ISSC-2022 Committee III.1-Ultimate strength benchmark study on the ultimate limit state analysis of a stiffened plate structure subjected to uniaxial compressive loads. *Marine Structures*, 79, 1-26.

Paik, JK. and Kim, BJ. (2002). Ultimate strength formulations for stiffened panels under combined axial load, in-plane bending and lateral pressure: a benchmark study. *Thin-Walled Structures*, 40(1), 45–83.

Georgiou, D. (2019). Buckling and Ultimate Strength of Stiffened Panels. Master Thesis. Norwegian University of Science and Technology, Norway.

Kolyvas, E., Drikos, L., Diamanti, E. and A. El Saer, AE. (2015). Application of photogrammetry techniques for the visual assessment of vessels' cargo hold. *Towards Green Marine Technology and Transport*, CRC Press, London.

Koelman, HJ. (2010). Application of a photogrammetry-based system to measure and re-engineer ship hulls and ship parts: An industrial practices-based report. *Computer-Aided Design*, 42, 731-743.

Tepegöz, A. (2019). Fotogrametrik yöntemle üç boyutlu gemi modelleme ve proje verileri ile karşılaştırma. Master Thesis, Karadeniz Technical University, Trabzon, Türkiye.

Lloyd Register. (2016). ShipRight design and construction. Additional design procedures non-linear structural collapse analysis for plates and stiffened panels, 1-25.

Türk Loydu. (2019). Procedure for the determination of the ultimate strength of stiffened panels by using Non-Linear Finite Element Analysis. Technical Circular, İstanbul, Türkiye.

Chen, BQ., Garbatov, Y. and Soares, C.G. (2011). Automatic approach for measuring deformations in complex structures using photogrammetry technique. *Proceedings of the 22nd Pan American Conference of Naval Engineering, Maritime Transportation & Ports Engineering*, 1-18, Buenos Aires, Argentina.

Mouhat, O., Khamlichp, A. and Limam, A. (2013). Assessing buckling strength of stiffened plates as affected by localized initial geometric imperfections. *International Review of Applied Sciences and Engineering* 4(2).

Cubells, A., Garbatov, Y. and Soares, C.G. (2014). Photogrammetry measurements of initial imperfections for the ultimate strength assessment of plates. *Trans RINA, International Journal of Maritime Engineering, Part A4*, 156.

Zhang, S. (2015). A review and study on ultimate strength of steel plates and stiffened panels in axial compression. *Ships and Offshore Structures*. 11(1), 1-11.

Woloszyk, K., Bielski, PM., Garbatov, Y., Mikulski, T. (2021). Photogrammetry image-based approach for imperfect structure modelling and FE analysis. *Ocean Engineering*, 223, 1-14.

Woloszyk, K., Garbatov, Y., Kowalski, J. and Samson, L. (2020). Experimental and numerical investigations of ultimate strength of imperfect stiffened plates of different slenderness. *Polish Maritime Research*, 27(108), 120-129.

Graves, W., Nahshon, K., Aminfar, K. and Lattanzi D. (2023). Finite element model updating with quantified uncertainties using point cloud data. *Data-Centric Engineering*, 4(16), 1-19.

Barceló, AC. (2012). Structural assessment based on photogrammetry measurements and Finite Element Method. Master Thesis, Lisbon Technical University, Lisbon, Portugal.

Quinn, D., Murphy, A., McEwan, W. and Lemaitre, F. (2009). Stiffened panel stability behaviour and performance gains with plate prismatic sub-stiffening. *Thin-Walled Structures*, 47, 1457–1468.

ISSC (2012), Ultimate Strength (Committee III.1), Proceedings of the 18th International Ship and Offshore Structures Congress, Rostock, Germany, September.

Sekban, DM., Ölmez, H., Akterer, SM., Kose, E. and Pürçek, G. (2018). Effect of Friction Stir Processing on Ultimate Strength of Ship Hull Girder Plates Estimated by Finite Element Analysis, Proceedings of the 3rd International Naval Architecture and Maritime Symposium, Yıldız Technical University, Istanbul, Turkey, April 24-25, 2018.

ANSYS® Workbench™ R2022, User's Manual. <https://ansyshelp.ansys.com> [Online] [01-25.10.2023]

Photomodeler V.2023.3.0.238, User's Manual. <https://www.photomodeler.com/downloads/OnlineHelp/index.html> [Online] [01-25.10.2023]